Searching for the 1912 Maymyo earthquake: new evidence from paleoseismic investigations along the Kyaukkyan Fault, Myanmar

Author names and affiliations

Silvia Crosetto[1,*], Ian M. Watkinson[1], Soe Min[2], Emanuela Falcucci[3], Stefano Gori[3], Pyi Soe Thein[4], Sudeep[5]

[1] Department of Earth Sciences, Royal Holloway University of London, Egham, Surrey TW20 0EX, United Kingdom

[2] Department of Geology, Taungoo University, Bago Division, Myanmar

[3] Istituto Nazionale di Geofisica e Vulcanologia, Via di Vigna Murata, 605, 00143 Roma, Italy

[4] Department of Geology, University of Mandalay, Mandalay, Myanmar

[5] Department of Geology, University of Yangon, Yangon, Myanmar

Corresponding author

Silvia Crosetto (silvia.crosetto.2013@live.rhul.ac.uk);

**present address:* Helmholtz-Zentrum Potsdam, German Research Centre for Geosciences, GFZ, 14473 Potsdam, Germany

Abstract

The Great Burma earthquake (MsGR 8.0; Ms 7.6 - 7.7) occurred on May 23rd, 1912, and was one of the most remarkable early 1900's seismic events in Asia as described by Gutenberg and Richter (1954). The earthquake, focused near Maymyo, struck the Northern Shan State in eastern Myanmar. Contemporary evaluation of damage distribution and oral accounts led to a correlation between the earthquake and the topographically prominent Kyaukkyan Fault near the western margin of the Shan Plateau, although direct evidence has never been reported. This study aims to find evidence of paleoseismic activity, and to better understand the relationship between the 1912 earthquake and the Kyaukkyan Fault. Paleoseismic trenching along the Kyaukkyan Fault revealed evidence of several surface rupturing events. The northernmost trench exposes at least two visible rupture events since 4660 ± 30 BP: an older rupture stratigraphically constrained by AMS ^{14}C dating to between 4660 ± 30 BP and 1270 ± 30 BP, and a younger rupture formed after 1270 ± 30 BP. The presence of pottery, bricks and cooking-related charcoal in the younger faulted stratigraphy demonstrates Kyaukkyan Fault activity within human times, and a possible correlation between the younger rupture and the 1912 Maymyo earthquake is not excluded. The southern paleoseismic trench, within a broad transtensional basin far from bounding faults, exposes two (undated) surface ruptures. Further study is required to correlate those ruptures to the events dated in the north. These preliminary paleoseismological results constitute the first quantitative evidence of paleoseismic activity along the northern ~170 km of the Kyaukkyan Fault, and support existing evidence that the Kyaukkyan Fault is an active but slow-slipping structure with a long interseismic period.

Keywords

paleoseismology; strike-slip fault; active tectonics; surface rupture; intraplate fault; calcrete

1. Introduction

The Kyaukkyan Fault is a N-S-trending ~500 km long, active right-lateral strike slip fault that lies on the western Shan Plateau, a region of almost 1 km average elevation in eastern Myanmar, western Laos and part of NW Thailand, located about 1000 km south of the Eastern Himalayan Syntaxis (Fig. 1a).

The Kyaukkyan Fault is generally considered to have been the origin of a large earthquake that hit northern Myanmar on 23rd May 1912, based on contemporary damage mapping (Coggin Brown, 1917; Fig. 1b). This mapping focused on damage to buildings, railway infrastructure, ground effects such as cracks and gravitational processes and modification of the underground water network, corresponding to intensity IX of the Rossi-Forel scale where maximum intensity is intensity X. The Maymyo earthquake (Maymyo is a city in Shan State more recently known as Pyin Oo Lwin) was initially estimated at MsGR 8 (Gutenberg and Richter, 1954), and more recently revised to Ms 7.7 to 7.6 (e.g Abe and Noguchi, 1983; Pacheco and Sykes, 1992). Wang et al. (2014) re-evaluated the distribution of highest intensities, and, together with the inferred magnitude of the earthquake, concluded that the 1912 event likely ruptured the entire 160 km-long northern section of the Kyaukkyan Fault.

Despite the isolated 1912 event, the Kyaukkyan Fault has been largely devoid of significant seismicity (e.g. Chhibber and Ramamirtham, 1934; Le Dain et al., 1984; Wang et al., 2014; Soe Min et al., 2017). However, there has been modern strike-slip activity across the broader Shan Plateau, including the Mw 6.8 Tarlay event in March 2011 (see Fig. 1a; Soe Thura Tun et al., 2014). A recent study of tectonic landforms and related Quaternary deposits along the Kyaukkyan Fault (Crosetto et al., 2018) revealed distinctive geomorphologic and structural features, indicative of strongly transtensional strike-slip during the Quaternary. That study provided the background for the identification of two suitable paleoseismic trenching sites.

The few published paleoseismic trenching studies in Myanmar have so far been limited to the Sagaing Fault (e.g. Wang et al., 2011). There have also been extensive paleoseismic surveys in northern Thailand (e.g. Fenton et al., 2003; Kosuwan et al., 1999; Morley et al., 2011 and references therein). This study aims to redress the deficiency in paleoseismic knowledge of the Kyaukkyan Fault to provide evidence for its

Holocene activity and potential involvement in the 1912 earthquake. Future study of the Kyaukkyan Fault should further clarify to the tectonic evolution and seismic hazard of eastern Myanmar, and the behaviour of the complex plate boundary between India and Sundaland.

2. Geologic overview

2.1. Tectonic setting

The Kyaukkyan Fault bisects the western Shan Plateau, which is the southernmost promontory of Tibetan Plateau elevated topography (Fig. 1c). The fault lies within Sibumasu, a Gondwana-derived terrane accreted to Eurasia during the Paleozoic as part of the assembly SE Asia's continental core, termed Sundaland (e.g. Metcalfe, 1984, 2013). The Cenozoic tectonics of Myanmar have been dominated by northward indentation of Indian continental crust into Asia (e.g. Tapponnier et al., 1982; Treloar and Coward, 1991; van Hinsbergen, 2011), associated increasingly oblique subduction of Indian oceanic crust beneath western Sundaland (e.g. Lee and Lawver, 1995; Nielsen et al., 2004; Curray, 2005), and effects of Tibetan Plateau crustal thickening and gravitational collapse (e.g. Rangin et al., 2013). During the Late Oligocene to Early Miocene, India coupled with western Myanmar (e.g. Curray et al., 1979; Curray, 2005; Searle and Morley, 2011) detaching it from stable Sibumasu (Morley, 2009), and moved north relative to Sundaland, establishing a belt of dextral transpression focused on Myanmar that continues to the present (e.g. Molnar and Tapponnier, 1975; Curray et al., 1979; Bertrand and Rangin, 2003; Vigny et al., 2003; Soe Thura Tun and Watkinson, 2017).

The current convergence rate between India and Eurasia is 43 mm/yr (Socquet and Pubellier, 2005; Vigny et al., 2003); relative motion between India and stable Sundaland is 35-36 mm/yr, of which about half is accommodated by the N-S-trending Sagaing Fault (Socquet et al., 2006), the most prominent strike-slip fault in Myanmar. Residual motion may be accommodated partly in the Indo-Myanmar Ranges, in the West Andaman fault system, and the remainder distributed within the Shan Plateau (e.g. Sahu et al., 2006; Socquet et al., 2006; Vigny et al., 2003). The latter may include a partition across the Kyaukkyan Fault, possibly in the order of 1 mm/yr based on large river offsets (Wang et al., 2014) or up to 9-18 mm/yr based on displacement of manmade artefacts (Soe Min et al., 2017), reported below in the text.

2.2. Quaternary evolution of the Kyaukkyan Fault

The Quaternary evolution of the Kyaukkyan Fault has been documented by Crosetto et al. (2018). Quaternary deposits such as alluvial fans are faulted and display small scale folding particularly along the eastern basin-bounding fault of Inle Lake basin, showing evidence of transtension, transpression and pure strike-slip. Youthful stream offsets and deflections characterise the northern section of the fault – the maximum robust stream offset is ~1560 m to the right, while offset restoration for a population of 28 streams gave a best fit of 125 m dextral offset.

The ancient Pawritha city wall straddles the Kyaukkyan Fault north of Inle Lake (Fig. 1c), and is apparently offset to the right by 12.2 ± 1.8 m (Soe Min et al., 2017). The measurement is based on the trace of an ancient wall marked by brick-cored embankments and highlighted by a road to the south. Given the inferred 9th to 13th Century age of the wall (Moore, 2007), this displacement would yield a high slip rate of 10 mm/yr. However, it has to be considered that measurement of the displacement is necessarily imprecise and does not take into account the possibility that part of the construction might have crumbled over a wider area. Uncertainty also exists about the exact age of the original wall.

Historic activity of the Kyaukkyan Fault is also testified by records of historic and instrumental-era seismicity and by the Mandalay-Lashio railway which, following the 1912 Maymyo earthquake, was "*bent into a smooth curve close to the actual line of the* [Kyaukkyan] *fault*" at Kyaukkyan village (Coggin Brown, 1917). The railway bend is a key line of evidence linking that earthquake to the Kyaukkyan Fault (e.g. Soe Min, 2010; Wang et al., 2014, 2009). However, the well-used modern rails and embankments have clearly been maintained in the last century and it remains unclear to what extent the present-day engineered curve replicates the co-seismic bending observed by Coggin-Brown soon after the 1912 earthquake. It is also unclear if the modern curve replicates any pre-earthquake engineered curve, or whether the line was built perfectly straight, since there are no records of sufficient detail (Crosetto et al., 2018).

3. Methods

Paleoseismic trenching sites across the Kyaukkyan Fault were identified after extensive mapping of Quaternary geomorphic features along the fault system (Crosetto et al., 2018), through field observations and by interpretation of 90 m Shuttle Radar Topography Mission (SRTM) digital topographic data, 30 m ASTER Global Digital Elevation Model (GDEM), 2.5 m SPOT and 1 m DigitalGlobe imagery accessed via Google Earth and the ESRI World Imagery compilation. Reconnaissance field observations were the basis for more detailed site investigation and topographic mapping preceding the trenching works.

Trenches were dug across N-S-trending lineaments representing possible superficial expression of the Kyaukkyan Fault in order to identify evidence of past faulting and rupturing events within the stratigraphic record.

Absolute age control on the stratigraphy was obtained by AMS ^{14}C radiocarbon dating on three charcoal samples collected from trench T1 in March 2016. Samples were collected within host clays, wrapped in aluminium foil, dried and sealed in plastic bags. Transmitted light microscopy to identify the best material was conducted under clean conditions. AMS analyses were performed at BETA Analytic in July 2017. BetaCal3.21 and the INTCAL13 curve (Reimer et al., 2013) were used for AMS ^{14}C ages calibration. Radiocarbon results are reported in Appendix A, according to the standard convention defined by Millard (2014).

In the following descriptions, ‘N-wall’ and ‘S-wall’ will be used to indicate the northern and the southern walls of all E-W-trending trenches.

4. Paleoseismological observations

4.1. Trench T1

Trench T1 is located close to Kyaukkyan village, north of the Mandalay-Lashio railway bend described by Coggin Brown (1917). The area is characterised by generally flat topography (Fig. 2a), bounded to the west by a narrow N-S-trending ridge of grey limestone belonging to the Ordovician Naunghkangyi Group and showing intense fracturing and faulting. A scarp marks the transition from the bedrock to the alluvial plain, which is occupied by cultivated fields. Away from the ridge, there is no natural outcrop, but in all trenches and in a number of other artificial pits, the carbonate bedrock lies immediately below a thin, *terra rossa*-type soil. There is no regolith, and the top of the carbonate is smooth and composed of highly indurated, crystalline limestone, cut by numerous shear fractures and faults.

Parallel to the ridge, below the eastern scarp, two subtle ~N170E-trending lineaments 100 - 200 m long are visible in the topography. The easternmost lineament is defined by aligned sag ponds (Fig. 2b) and *en échelon* linear features, interpreted as rupture segments, which delimit metric zones of subsidence highlighted by difference in vegetation (Fig. 2c). Two preliminary trenches dug across the *en échelon* segments revealed very shallow bedrock characterised by generally ~N30E-trending fractures dipping toward the west with average dip angle of 40°. There was no evidence of surface rupture in the thin soil above the bedrock. The entire succession was likely to have been disturbed by agricultural activity.

The westernmost and more prominent lineament is expressed, 1 km north of the railway bend at Kyaukkyan village, as aligned subsiding areas of circa 100 m^2 and decametric dolines in the limestone; further south the lineament has a topographic relief of <1 m highlighted by vegetation and soil colour contrast, picked out by boggy areas rich in decaying organic material (Fig. 2d). Along the same lineament south of the railway is a sharp, linear soil colour difference given by the juxtaposition of grey soil to the west and *terra rossa* soil to the east (Fig. 2e).

The 19th-century Mandalay-Lashio railway passes through a blasted notch in the limestone ridge and, east of the scarp, continues along a man-made embankment ~5 m wide and standing ~2 m above surrounding fields. The line is straight where it passes through the limestone ridge and is smoothly bent to the right where it crosses the open plain, orthogonal the fault trend (Fig. 2d, e). Although the railway embankment also appears to be deflected in the same way, it is largely obscured by vegetation. The deflected railway line continues east for ~100 m until the tracks bend northwards at Kyaukkyan village.

Assuming an initial straight geometry of the railway tracks from where they exit the limestone ridge towards the village, we measured the right-lateral deviation from the projected straight line in 5 m increments (Fig. 2f, g). The measurements, reported in Fig. 2f, yield a total deviation from the straight projected line of 2.0 ± 0.2 m. On the basis of the topographic lineament and assuming that the apex of the railway line bend marks the 1912 surface rupture, trench T1 was dug 250 m north of the railway, across the lineament and the topographic high (see Fig. 2d).

4.1.1.Stratigraphy

The trench was perpendicular to the westernmost lineament, and orientated N80E along its 17 m length. The trench wall grid and logs were numbered from m 0 to m 17 from east to west. The westernmost part (m 14 to m 10) of the trench was <1 m deep, due to a hard calcareous layer that impeded deeper excavation (Fig. 2h). This section, closer to the mountain front, was characterised by generally continuous calcrete layers alternating with hard, calcified silt. Calcrete is a calcium carbonate duricrust precipitated from carbonate-rich groundwaters in times of aridity. It acts to cement components of soil or rock, and can form non-stratiform deposits.

A softer portion of the hard calcareous layer caused the formation of a step at m 10, deepening the base of the trench by 1.3 m, and reaching ~1.8 m depth. In this eastern section the trench walls exposed a succession of alternating clay paleosoils with calcrete layers illustrated in Fig. 3. The terms used in this section to describe the calcrete stratigraphic horizons refer to the schematic idealised pedogenic profile proposed by Alonso-Zarza and Wright (2010; after Esteban and Klappa, 1983). Below the agricultural layer, we distinguished the following units as schematically reported in the trench logs of Fig. 4a, b:

- B3: only found on the N-wall, it represents the upper calcrete, characterised by a centimetric platy horizon with well-defined laminae containing “alveolar” honeycomb weathering structures and tubiform pores. It is separated from the underlying calcrete B2 by a chalky-nodular layer t2 with abundant carbonate powder and carbonate grains from millimetric to 0.5-1 cm, and locally more clayey. B3 and B2 merge at m 4 where, on the N-wall, abundant charcoal arranged as the shape of a pot suggests a cooking/baking pit (Fig. 5a). B3 and B2 are truncated at m 3. B3 was not identified on the S-wall, where there is probably vertical continuity between B2 and B3.

- B2: platy calcrete with prominent lamination, wavy to thinly bedded, forming continuous layers on both walls; it is laterally truncated at m 3 and at m 2.6 in the N- and S-wall, respectively. On the N-wall B2 is also encompasses a lower second layer of calcrete, 1.5 m long and ending at m 8. These two branches of B2 are separated by a darker, nodular horizon, composed of indurated, centimetric nodules in a less carbonate-rich matrix.
- C2: clay, dark brown, homogeneous. Contains sparse millimetric, subrounded grains of bricks, calcrete, charcoal and pisoids that appear organised in a layer <10 cm thick between m 4 and m 6.5 in the S-wall. 'Flames' of light-brown clay material are found around m 3 in the S-wall. C2 is found geometrically above and below units B2+B3 as it acted as host rock for precipitation of the upper calcrete layers.
- B1.b: chalky calcrete observed on the N-wall. It is characterised by soft micrite with abundant grains and pisoids. At the top, a discontinuous platy horizon is locally substituted by a nodular horizon, characterised by 1.5 mm in size, sub-rounded, indurated carbonate nodules. At the easternmost termination of the layer a well defined platy horizon shows at least 15 cm of millimetric laminae. Portions of transition layer t1, separating B1.b from B1.a, are darker and fine-grained, and the clay content is greater than the carbonate content.
- B1.a: at the base of t1, this unit is more prominent on the S-wall, where it appears as a nodular to platy calcrete layer, laterally truncated at m 3. On the N-wall it is a thin, discontinuous layer in the western part and more continuous toward the east at m 5.
- C1: lowermost clay, chestnut brown colour, homogeneous with mm to cm dark stains, probably altered carbonate.

At the easternmost end of the trench a red brick layer lay 80 cm below the surface within unit C2 (Fig. 5b). The sub-horizontal brick layer, 20 cm thick and about 1 m wide, appeared as the base of a built structure though there was no evidence that it was in-situ. The brick material was soft and friable.

The sedimentary succession mapped on the trench walls was cross-cut by four main discontinuities interpreted as N-S-trending faults (see Fig. 4a, b). On the N-wall the easternmost faults *F3* and *F4* folded units B1 and B2+B3, creating a geometric vertical step along the layers (Fig. 5c), and truncated the eastern termination of the calcrete layer B2+B3 (Fig. 5d). On the southern wall only the calcrete layer B2 appeared truncated by *F6,* which is interpreted to correlate across the trench to *F4*. On the N-wall the westernmost two faults *F1* and *F2* juxtaposed along a sharp lateral contact units B1.b and t1, with the top of B1.b appearing irregular along both fault traces. On the S-wall B1.a was characterised by open fractures, putting into contact the clay units C1 and C2, that may correspond to a fault trace *F5,* interpreted to correlate to *F1* or *F2* across the trench.

4.1.2. Radiocarbon dating and paleoearthquake interpretation

Thirty-two samples of charcoal and shell fragments were collected from key stratigraphic horizons, from which three charcoal fragments were selected for radiocarbon dating (Table 1). Sample KT201-C24, in the upper layer of unit B2 in the N-wall of the trench, yielded a radiocarbon age of 1270 ± 30 BP. Sample KT201-C04, at the top of unit t1 in the S-wall, yielded an age of 4660 ± 30 BP. Sample KT201-C15, collected 15 cm below the contact between units B1.a and C1 from the S-wall, yielded an age of 8670 ± 60 BP.

Table 1. ^{14}C Dating of charcoals from trench T1[a]

Sample Name	Trench Unit	Amount of Carbon (mg)	d13C (‰)	Radiocarbon age (BP)	Uncertainty (±years)	Calibrated Age 2σ Range
KT201-C24	B2	2.6	-26.4	1270	30	662-778[b] AD
KT201-C04	B1	1.76	-22.3	4660	30	3519-3365[c] BC
KT201-C15	C1	27.4	-26.5	8670	60	7848-7582[b] BC

[a] 2σ range, 95.4% probability density
[b] Reported value: 92.3% probability density
[c] Reported value: 95.4% probability density

On the S-wall, the brick layer within unit C2 lies stratigraphically below the calcrete layer B2, where a charcoal sample yielded an age of 1270 ± 30 BP, corresponding to the end of the 7^{th} century AD. Bricks and terracotta plaques have been found along Myintnge and Zawgyi river valleys and within Inle basin and dated to the early centuries CE (Moore, 2009; Moore and Myint, 1991), potentially confirming the measured age of the newly excavated Kyaukkyan artefacts (E. Moore, pers. comm. 2017).

The relation between stratigraphic units and deformation allowed to distinguish at least two events, constrained by radiocarbon ages: 1) folding of units B1-B3 and clear truncation of unit B2 constrains a younger rupture event after 1270 ± 30 BP, equivalent to 680 ± 30 AD; 2) an older rupture event juxtaposes units B1.b and t1 across faults *F1* and *F2*, and is sealed by unit B2, constraining the rupture to before 1270 ± 30 BP. This rupture cuts all older units up to the t1/C2 contact, dated to 4660 ± 30 BP, and so must be younger than that age, i.e. constrained between 1270 ± 30 BP to 4660 ± 30 BP. The lack of correlation between displaced horizons does not allow to infer slip rates along the observed fault traces.

4.2. Trench T2

Trench T2 was located north of Taunggyi city. The trench site was identified by a ~500 m long linear N-S-trending feature between two forested areas, highlighted by the contrast between lighter and darker sediment in 2012 DigitalGlobe/Google Earth imagery. The lineament lies about 100 m west of a gentle 1 m high scarp, which separates grey basin-filling sediment from a flat area, gently dipping west and from the mountain front ~2 km to the east (Fig. 6a). The scarp was interpreted as the expression of a fault synthetic to the basin-bounding fault in the shallow subsurface (Crosetto et al., 2018). The flat, 'terraced' area is covered with *terra rossa*, inferred to be an alteration product overlying shallow buried banded limestone, sporadically exposed along the basin margin.

Field observations revealed that the lineament mainly reflected different water saturation of the basin-filling sediment, and was initially interpreted as a seismically triggered sand blow. A detailed topographic survey highlighted a gentle scarp at the southern termination of the lineament, and a pilot trench dug across this scarp exposed at least 1.5 m of water-saturated peat (Fig. 6b); however, no clear stratigraphy or evidence of deformation was observed in the pilot trench. The instability of the walls required the trench to be closed, and further examinations of the walls could not be undertaken. Trench T2 was subsequently opened across the 1 m scarp between the basin and the terraced area (Fig. 6b).

4.2.1. Stratigraphy

Trench T2 was orientated N116E, was 7.3 m long and 1.2 m wide. It exposed a 1.5-2 m succession mainly characterised by clay units, schematically represented in the trench logs of Fig. 7a, b. The description of units and faulting events follows a relative chronology criterion, since deep roots contaminated any datable material.

From the top, a thin layer of dry soil lies above the agricultural layer, which has a constant thickness of 40 cm, it is darker and drier than the underlying units and contains centimetric fragments of bricks. The uppermost clay C2 is dark brown in colour, homogenous and hard; on the N-wall abundant fragments of modern pottery defined the shape of a hole dug into the ground. Below C2, the clay unit C1 has chestnut brown colour (Fig. 8a); it is divided into an upper unit C1a, fine, well sorted, with plastic rheology, and a lower unit C1b, generally coarser, containing millimetric pisoids. Roots and root marks were visible on both walls within units C1 and C2. The base of the trench was dolomitic limestone with closely-spaced subvertical fractures showing an average strike of N45E (Fig. 8b).

The sedimentary succession mapped on the two trench walls was cross-cut by four main discontinuities that are interpreted as N-S-trending faults. Trench T2 was narrower than trench T1, so correlations between north and south walls could be made with confidence. To the west on the N-wall, the youngest faults *F3* and *F4* were highlighted by lateral contact of unit C1b with C2 along *F4*, and of unit C1a with C2 and C1b along *F3*. The faults' correlatives on the S-wall had a less pronounced offset across them. No deformation was visible above unit C2. Older surface ruptures were represented by *F1* and *F2*, where fault gouge derived from the dolomitic limestone was gradually mixed with the lower part of C1b (Fig. 8c).

5. Discussion

5.1. Evaluation of trenching results

Paleoseismic trenching along the northern and central section of the Kyaukkyan Fault provides the first robust evidence of paleoearthquakes that have occurred along the fault and their timing.

In the northern site at Kyaukkyan village we were particularly searching for evidence of the 1912 earthquake described by Coggin Brown (1917), and for this reason we dug trench T1 across a lineament along strike from the reportedly co-seismic railway bend (Fig.9). Radiocarbon dating of charcoal grains constrains at least two potential rupture events, expressed in the trench as offset and/or truncated horizons. The validity of this interpretation is subject to the correct interpretation of discontinuities that truncate and irregularly offset laterally continuous layers observed in the trench as faults or surface ruptures.

Calcrete layers, the main stratigraphic markers truncated in the trench, show characteristic features of pedogenic precipitation of $CaCO_3$ from groundwater. The carbonate precipitates along stratigraphic horizons, preferably in those with higher permeability, and creates flat layers that tend to pick out the shape of the sedimentary unit where they precipitate. The pattern of abrupt lateral truncation described above, in particular the non-systematic pattern of stratigraphic displacement, could also be explained by laterally discontinuous pedogenic calcrete precipitation or erosion, for example during terrace aggradation (e.g. Candy et al., 2003) or due to gravitational processes. However, we observed no evidence of these processes in the host clay units. Moreover, the stratigraphic folding often associated with the discontinuities, their generally steep/listric dips and the easy correlation of major fault F4-F6 across trench T1 to define a N-S-trending structure lend support to our interpretation that the discontinuities are most likely fault-related surface ruptures. In particular, large strike-slip earthquakes by their nature generate wide, complex 3-dimensional patterns of vertical and lateral offsets (e.g. Barka et al. 2002; Haeussler et al. 2004; Fu et al. 2005) that can explain the observed irregularities in layer thickness and difficulties with dip-slip restoration in the 2-D trench walls.

5.2. Which fault strand?

A strike-slip fault can cause long horizontal displacements that normally occur on one or multiple strands. Consequently, trenching on a strike-slip fault can be challenging as a single strand might not necessarily record all the paleoearthquakes that occurred along that section of the fault (Keller and Pinter, 1996; McCalpin, 2009).

Trench T1 at Kyaukkyan village was selected because of its proximity to the railway offset reported by Coggin Brown (1917), which was previously the only line of evidence of the location of surface rupture during the 1912 earthquake. The bend lies across a fault strand that is subtly expressed as a change in colour and topography of the agricultural soil. The youngest rupture event identified in the trench occurred between 1270 ± 30 BP and present, including the possibility that the observed rupture corresponds to the 1912 earthquake. However, to exclude coincidence, a 1912 interpretation remains strongly dependent on the interpretation of the railway bend, that lies directly along strike from the trench and its ruptures, as a fault offset. Since it is unclear whether the railway curvature is tectonically-induced or man-made, several different scenarios could be argued:

- the railway bend and the ruptures mapped in trench T1 are coseismic features that both formed during the 1912 earthquake;
- the rupture identified in the trench formed during the 1912 earthquake, but the railway bend as observed by Coggin-Brown (1917) has been lost due to subsequent rebuilding, and the present curve is an engineered structure that imperfectly mimics fault offset;
- the rupture in the trench corresponds to an earthquake older than 1912 but younger than 1270 ± 30 BP, meaning that our trench did not intercept the segment that failed in 1912 and that the railway bend has always been an engineered curve;
- the rupture is a discontinuity due to secondary effects of an earthquake that occurred elsewhere any time after 1270 ± 30 BP and including 1912, such as gravitational processes induced by ground shaking. The source could be another strand of the Kyaukkyan Fault, or another fault entirely (e.g. Sagaing Fault). The railway bend could be an engineered curve or may have been the result of off-fault gravitational processes.

The southern trench T2 exposed a faulted wedge that, although undated, testifies the existence of recent fault activity far from the main basin-bounding faults, as proposed by Crosetto et al. (2018). This finding, whilst not excluding the possibility of coeval fault rupture along the basin-bounding faults, confirms that recent Kyaukkyan Fault earthquake ruptures may have traversed the transtensional basin and may lack prominent geomorphic expression. A similar property was demonstrated by the 2018 Mw7.5 Palu earthquake, Indonesia, in which the surface rupture mostly crossed alluvial fans well east of topographically prominent basin-bounding structures (Socquet et al., 2019). This tendency of large strike-slip earthquakes to bypass basin sidewall structures has important implications for paleoseismic investigations, which may miss large paleo-earthquakes in transtensional settings.

5.3. Geodetics and seismicity

Of the total 35-36 mm/yr geodetic motion of the Indian plate with respect to Sundaland, in Myanmar the Sagaing Fault accommodates ~18 mm/yr of right-lateral strike-slip, while the remainder is accommodated within the Arakan Trench, in the Indo-Myanmar Ranges and other structures across Myanmar (e.g. Vigny et al., 2003; Socquet et al., 2006). A GPS station located west of the Kyaukkyan Fault indicates 6 mm/yr westward motion with respect to the Sunda Plate over two years of measurements, and a station at Taunggyi to the east indicates 4 mm/yr south-westward motion (Socquet et al., 2006), reflecting a possible diffuse deformation across the fault. However, the poor GPS network coverage on the Shan Plateau limits further speculation about the Kyaukkyan Fault's modern slip behaviour.

The instrumental seismic record shows that the Kyaukkyan Fault has been devoid of large seismic events (IRIS and NEIC catalogues, USGS, 2018). Assuming the 1912 earthquake was caused by the Kyaukkyan Fault, it is the only significant event recorded along its length. Distributed seismicity affects the Shan Plateau but only a few events, of $M<5$, are located within the Kyaukkyan fault system. Linking the 1912 event to the Kyaukkyan Fault is thus critical to distinguishing whether its characteristic behaviour can be approximated as slow creeping or as stick-slip with large infrequent earthquakes with an interseismic period longer than 100 years.

5.4. Potential earthquake scenarios

Assuming the 1912 earthquake attained magnitude 7.7 to 7.6 (e.g Abe and Noguchi, 1983; Pacheco and Sykes, 1992) and ruptured the northern 160 km of the Kyaukkyan Fault (Wang et al. 2014), then maximum displacement could have reached about 8-9 m, according to empirical relationships derived by Wells and Coppersmith (1994). Recent large strike-slip earthquakes of similar size have developed well documented displacement maxima of 7.9 m (M7.9 Kunlunshan, 2001; Xu et al. 2002); 8.8 m (M7.9 Denali Fault, 2002;

Haeussler et al. 2004); 13.6 m (M7.7 Balochistan, 2013; Gold et al. 2015); and 7 m (M7.5 Palu Fault, 2018; Socquet et al. 2019). All of these offsets are discordant with the apparent railway offset at Kyaukkyan (2.0 ± 0.2 m), although peak displacements in all cases above were complexly distributed along the faults and not necessarily close to earthquake epicentres. It is also not clear exactly where the 1912 earthquake originated or in which direction rupture propagated, which will impact offsets at specific locations. Taking 7-8 m as a conservative estimate for the Maymyo event peak surface displacement and assuming a characteristic earthquake model, the Kyaukkyan Fault would require a 7-8 ka interseismic period for similar repeated events if slipping at 1 mm/yr, or 400-900 years if slipping at 9-18 mm/yr. Our paleoseismic results suggest at least two surface rupturing earthquakes within the last 4660 ± 30 years. Taking a very crude average of one characteristic earthquake similar to 1912 per 2330 years yields a slip rate of 3-3.4 mm/yr, broadly consistent with the sparse geodetic observations on the western Shan Plateau. This long interseismic period is also consistent with the observation that the Kyaukkyan Fault has generated little seismicity since 1912, and there were no historical records of earlier events.

Several workers have commented on the conspicuous tectonic geomorphology of the Kyaukkyan Fault and numerous associated structures (e.g. Morley 2009; Wang et al. 2009; Soe Min 2010; Wang et al. 2014; Soe Min et al. 2017; Crosetto et al. 2018), some of which (e.g. Mae Ping Fault, Shan Scarp Fault) are known to record a pre-Miocene history far older than the current locus of dextral shear in Myanmar, the Sagaing Fault (see reviews in Morley et al., 2011 and Soe Thura Tun and Watkinson, 2017). On this basis it can be proposed that the Kyaukkyan Fault is a site of long-lived lithospheric weakness that is currently ~50 km inboard of the geodetic boundary occupied by the rapidly-slipping Sagaing Fault. While the Kyaukkyan Fault accommodates relatively little tectonic strain, it is suitably oriented and structurally mature enough to be occasionally reactivated and generate very large earthquakes. For hazard assessment it should also be considered that the Kyaukkyan Fault is one of several similar structures on the Shan Plateau, which may individually rupture infrequently, but as a population may have a much shorter interseismic period.

Further study is required to fully attribute the 1912 earthquake to the Kyaukkyan Fault, to determine its rupture length and peak displacement, to gather additional evidence for the ≤4660 ± 30 event we have identified that preceded it, and to more fully understand the distribution of tectonic strain across the numerous N-S-trending structures of the western Shan Plateau.

6. Conclusions

- The first paleoseismic trenches along the Kyaukkyan Fault reveal evidence of surface rupturing events along its northern and central sections.
- The northern trench exposes at least two visible rupture events: an older one, stratigraphically constrained by AMS ^{14}C dating to between 4660 ± 30 BP and 1270 ± 30 BP, and a younger one between 1270 ± 30 BP and the present.
- Although direct evidence for the 1912 M7.7-7.6 Maymyo earthquake was not found, the rupture younger than 1270 ± 30 BP may well correspond to that early 20th Century event, particularly as it lies directly along strike from the railway bend first noted after that earthquake. Additionally, the presence of pottery, brick fragments, a cooking pit and charcoal in the faulted stratigraphy demonstrates activity of the Kyaukkyan Fault within human times.
- The southern trench far from bounding faults within a broad transtensional basin exposes two surface ruptures. Further study is required to correlate that rupture to the events dated in the north.
- These preliminary paleoseismic results are consistent with existing evidence that the Kyaukkyan Fault is active, and point to a relatively long interseismic period for its northern/central segments. Resolution of the radiocarbon dating was insufficient to constrain that period to anything better than the order of hundreds to thousands of years.
- The Kyaukkyan Fault passes through or close to Shan State capital city Taunggyi, booming tourist centres Nyaungshwe and Pyin Oo Lwin, and is only 70 km from Myanmar's second largest city Mandalay. A repeat 1912-style earthquake would cause unprecedented devastation in the country, and remaining questions about the fault's history and seismic hazard should be addressed urgently.

Acknowledgements

Funding for this research was provided by the Kirsty Brown Memorial Fund, the Santander Travel Award, the Royal Holloway Reid Scholarship and the Department of Earth Sciences Research Committee. We would like to thank Dr Lin Thu Aung and Dr Myo Thant for their logistical support, and Kaung Si Thu, Myat Min, Than Soe, and Mr Naing for valuable support in the field. Prof. Elizabeth Moore is thanked for sharing her knowledge about artefacts found on the Shan Plateau. We thank two anonymous reviewers for their useful comments that improved this manuscript.

References

Abe, K., Noguchi, S.I., 1983. Revision of magnitudes of large shallow earthquakes, 1897-1912. Phys. Earth Planet. Inter. 33, 1–11.

Alonso-Zarza, A.M., Wright, V.P., 2010. Calcretes. Dev. Sedimentol. 61, 225–267.

Barka, A., Akyüz, H.S., Altunel, E., Sunal, G., Cakir, Z., Dikbas, A., Yerli, B., Armijo, R., Meyer, B., De Chabalier, J.B., 2002. The surface rupture and slip distribution of the 17 August 1999 Izmit earthquake (M 7.4), North Anatolian fault. Bull. Seismol. Soc. Am. 92, 43–60.

Bertrand, G., Rangin, C., 2003. Tectonics of the western margin of the Shan Plateau (central Myanmar): Implication for the India-Indochina oblique convergence since the Oligocene. J. Asian Earth Sci. 21, 1139–1157.

Candy, I., Black, S., Sellwood, B.W., Rowan, J.S., 2003. Calcrete profile development in Quaternary alluvial sequences, southeast Spain: implications for using calcretes as a basis for landform chronologies. Earth Surf. Process. landforms 28, 169–185.

Chhibber, H.L., Ramamirtham, R., 1934. The geology of Burma. MacMillan, London.

Coggin Brown, J., 1917. The Burma Earthquake of May 1912: Mem. Geol. Surv. India 42, 1–147.

Crosetto, S., Watkinson, I.M., Soe Min, Gori, S., Falcucci, E., Nwai Le Ngal, 2018. Evidence of Quaternary and recent activity along the Kyaukkyan Fault, Myanmar. J. Asian Earth Sci. 156, 207–225.

Curray, J.R., 2005. Tectonics and history of the Andaman Sea region. J. Asian Earth Sci. 25, 187–232.

Curray, J.R., Moore, D.G., Lawver, L.A., Emmel, F.J., Raitt, R.W., Henry, M., Kieckhefer, R., 1979. Tectonics of the Andaman Sea and Burma: convergent margins, in: Watkins, J., Montadert, L., Dickenson, P.W. (Eds.), Geological and Geophysical Investigations of Continental Margins. American Association of Petroleum Geologists Special Volumes, pp. 189–198.

Esteban, M., Klappa, C.F., 1983. Subaerial exposure environments, in: Scholle, P.A., Bebout, D.G., Moore, C.H. (Eds.), Carbonate Depositional Environments. American Association of Petroleum Geologists Memoir, pp. 1–96.

Fenton, C.H., Charusiri, P., Wood, S.H., 2003. Recent paleoseismic investigations in Northern and Western Thailand. Ann. Geophys. 46.

Fu, B., Awata, Y., Du, J., Ninomiya, Y., He, W., 2005. Complex geometry and segmentation of the surface rupture associated with the 14 November 2001 great Kunlun earthquake, northern Tibet, China. Tectonophysics 407, 43–63.

Gold, R.D., Reitman, N.G., Briggs, R.W., Barnhart, W.D., Hayes, G.P., Wilson, E., 2015. On-and off-fault deformation associated with the September 2013 Mw 7.7 Balochistan earthquake: Implications for geologic slip rate measurements. Tectonophysics 660, 65–78.

Gutenberg, B., Richter, C.F., 1954. Seismicity of the Earth and Associated Phenomena, 2nd ed. Princeton University Press, Princeton, N.J., USA.

Haeussler, P.J., Schwartz, D.P., Dawson, T.E., Stenner, H.D., Lienkaemper, J.J., Sherrod, B., Cinti, F.R., Montone, P., Craw, P.A., Crone, A.J., 2004. Surface rupture and slip distribution of the Denali and Totschunda faults in the 3 November 2002 M 7.9 earthquake, Alaska. Bull. Seismol. Soc. Am. 94, S23–S52.

Keller, E.A., Pinter, N., 1996. Active tectonics, 2nd ed. Prentice-Hall, Upper Saddle River, NJ, USA.

Kosuwan, S., Saithong, P., Lumchouan, A., Takashima, I., Charusiri, P., 1999. Preliminary results of paleoseismic studies on the Mae Ai Segment of the Mae Chan Fault Zone, Chiang Mai, Northern Thailand, in: The CCOP Meeting on Exodynamic Geohazards in East and Southest Asia, July. pp. 14–16.

Le Dain, A.Y., Tapponnier, P., Molnar, P., 1984. Active faulting and tectonics of Burma and surrounding regions. J. Geophys. Res. 89, 453–472.

Lee, T.-Y., Lawver, L.A., 1995. Cenozoic plate reconstruction of Southeast Asia. Tectonophysics 251, 85–138.

McCalpin, J.P., 2009. Paleoseismology, 2nd ed. Elsevier Inc., Amsterdam.

Metcalfe, I., 2013. Gondwana dispersion and Asian accretion: Tectonic and palaeogeographic evolution of eastern Tethys. J. Asian Earth Sci. 66, 1–33.

Millard, A.R., 2014. Conventions for reporting radiocarbon determinations. Radiocarbon 56, 555–559.

Molnar, P., Tapponnier, P., 1975. Cenozoic tectonics of Asia effects of a continental collision. Science (80- .). 189, 419–426.

Moore, E., 2009. Archaeology of the Shan Plateau: the Bronze to Buddhist transition. Contemp. Buddhism 10, 91–110.

Moore, E., 2007. Buddhist archaeology on the Shan plateau: the first millennium CE.

Moore, E., Myint, A., 1991. Finger-marked designs on ancient bricks in Myanmar. J. Siam Soc. 79, 81–102.

Morley, C.K., 2009. Evolution from an oblique subduction back-arc mobile belt to a highly oblique collisional margin: the Cenozoic tectonic development of Thailand and eastern Myanmar. Geol. Soc. London, Spec. Publ. 318, 373–403.

Morley, C.K., Charusiri, P., Watkinson, I.M., 2011a. Structural geology of Thailand during the Cenozoic., in: Ridd, M.F., Barber, A.J., Crow, M.J. (Eds.), The Geology of Thailand. Geological Society of London, London, pp. 273–334.

Morley, C.K., King, R., Hillis, R., Tingay, M., Backe, G., 2011b. Deepwater fold and thrust belt classification, tectonics, structure and hydrocarbon prospectivity: A review. Earth-Science Rev. 104, 41–91.

Nielsen, C., Chamot-Rooke, N., Rangin, C., 2004. From partial to full strain partitioning along the Indo-Burmese hyper-oblique subduction. Mar. Geol. 209, 303–327.

Pacheco, J.F., Sykes, L.R., 1992. Seismic moment catalogue of large shallow earthquakes, 1900 to 1989. Bull. Seismol. Soc. Am. 82, 1306–1349.

Rangin, C., Maurin, T., Masson, F., 2013. Combined effects of Eurasia/Sunda oblique convergence and East-Tibetan crustal flow on the active tectonics of Burma. J. Asian Earth Sci. 76, 185–194.

Reimer, P.J., Bard, E., Bayliss, A., Beck, J.W., Blackwell, P.G., Ramsey, C.B., Buck, C.E., Cheng, H., Edwards, R.L., Friedrich, M., 2013. IntCal13 and Marine13 radiocarbon age calibration curves 0–50,000 years cal BP. Radiocarbon 55, 1869–1887.

Sahu, V.K., Gahalaut, V.K., Rajput, S., Chadha, R.K., Laishram, S.S., Kumar, A., 2006. Crustal deformation in the Indo-Burmese arc region: Implications from the Myanmar and Southeast Asia GPS measurements. Curr. Sci. 90, 1688–1693.

Searle, M.P., Morley, C.K., 2011. Tectonics and thermal evolution of Thailand in the regional context of Southeast Asia, in: Ridd, M.F., Barber, A.J., Crow, M.J. (Eds.), The Geology of Thailand. Geological Society, London, pp. 539–572.

Socquet, A., Hollingsworth, J., Pathier, E., Bouchon, M., 2019. Evidence of supershear during the 2018 magnitude 7.5 Palu earthquake from space geodesy. Nat. Geosci. 12, 192.

Socquet, A., Pubellier, M., 2005. Cenozoic deformation in western Yunnan (China-Myanmar border). J. Asian Earth Sci. 24, 495–515.

Socquet, A., Vigny, C., Chamot-Rooke, N., Simons, W., Rangin, C., Ambrosius, B., 2006. India and Sunda plates motion and deformation along their boundary in Myanmar determined by GPS. J. Geophys. Res. Solid Earth 111, 1–11.

Soe Min, 2010. Structural study along the Kyaukkyan Fault, Shan State. University of Yangon.

Soe Min, Watkinson, I.M., Soe Thura Tun, Win Naing, 2017. The Kyaukkyan Fault, in: Geological Society (Ed.), Myanmar: Geology, Resources and Tectonics. London.

Soe Thura Tun, Wang, Y., Saw Ngwe Khaing, Myo Thant, Nyunt Htay, Yin Myo Min Htwe, Than Myint, Sieh, K., 2014. Surface Ruptures of the Mw 6.8 March 2011 Tarlay Earthquake, Eastern Myanmar. Bullettin Seismol. Soc. Am. 104, 2915–2932.

Soe Thura Tun, Watkinson, I.M., 2017. The Sagaing Fault, in: Barber, A.J., Ridd, M.F., Khin Zaw, Rangin, C. (Eds.), Myanmar: Geology, Resources and Tectonics. Geological Society of London Memoir, London.

Tapponnier, P., Peltzer, G., Le Dain, A.Y., Armijo, R., Cobbold, P.R., 1982. Propagating extrusion tectonics in Asia: New insights from simple experiments with plasticine. Geology 10, 611–616.

Treloar, P.J., Coward, M.P., 1991. Indian Plate motion and shape: constraints on the geometry of the Himalayan orogen. Tectonophysics 191, 189–198.

USGS, 2018. Search Earthquake Catalog [WWW Document]. IRIS NEIC Cat. ISC-GEM Glob. Instrum. Earthq. Cat. URL https://earthquake.usgs.gov/earthquakes/search/ (accessed 5.5.19).

van Hinsbergen, D.J.J., 2011. Short Note on the Use of Neotectonic and Palaeotectonic Nomenclature. Turkish J. Earth Sci. 20, 161–165.

Vigny, C., Socquet, A., Rangin, C., Chamot-Rooke, N., Pubellier, M., Bouin, M., Bertrand, G., Becker, M., 2003. Present-day crustal deformation around Sagaing fault, Myanmar. J. Geophys. Res. Solid Earth 108.

Wang, Y., Sieh, K., Soe Min, Khaing, S., Tun, S.T., 2009. Smoking gun of the May-1912 Burma earthquake? Neotectonics of the Kyaukkyan fault system, Eastern Burma (Myanmar), in: AGU. San Francisco, California.

Wang, Y., Sieh, K., Soe Thura Tun, Kuang Yin Lai, Than Myint, 2014. Active tectonics and earthquake potential of the Myanmar region. J. Geophys. Res. Solid Earth 119, 3767–3822.

Wang, Y., Sieh, K., Thura Aung, Soe Min, Saw Ngwe Khaing, Soe Thura Tun, 2011. Earthquakes and slip rate of the southern Sagaing fault: Insights from an offset ancient fort wall, lower Burma (Myanmar). Geophys. J. Int. 185, 49–64.

Wells, D.L., Coppersmith, K.J., 1994. New Empirical Relationships among Magnitude, Rupture Length, Rupture Width, Rupture Area, and Surface Displacement. Bull. Seismol. Soc. Am. 84, 974–1002.

Xu, X., Chen, W., Ma, W., Yu, G., Chen, G., 2002. Surface rupture of the Kunlunshan earthquake (Ms 8.1), northern Tibetan plateau, China. Seismol. Res. Lett. 73, 884–892.

Appendix A

REPORT OF RADIOCARBON DATING ANALYSES

Sample Information and Data	Sample Code Number	Conventional Radiocarbon Age (BP) or Percent Modern Carbon (pMC) & Stable Isotopes Calendar Calibrated Results: 95.4 % Probability High Probability Density Range Method (HPD)

Beta - 468809 — KT201-C04 / 467840 Supplement

Submitter Material: CHARCOAL mixed with clay
Analyzed Material: Charred material
Pretreatment: (charred material) acid/alkali/acid
Percent Modern Carbon: 55.98 +/- 0.21 pMC
Fraction Modern Carbon: 0.5598 +/- 0.0021
D14C: -440.16 +/- 2.09 o/oo
Δ14C: -444.68 +/- 2.09 o/oo (1950:2017)
Measured Radiocarbon Age: (without d13C correction): 4620 +/- 30 BP
Calibration: BetaCal3.21: HPD method: INTCAL13

4660 +/- 30 BP — IRMS δ13C: -22.3 o/oo

(95.4%) 3519 - 3365 cal BC (5468 - 5314 cal BP)

(68.2%):
(41.4%) 3476 - 3426 cal BC (5425 - 5375 cal BP)
(18.3%) 3508 - 3483 cal BC (5457 - 5432 cal BP)
(8.5%) 3382 - 3370 cal BC (5331 - 5319 cal BP)

Beta - 467841 — KT201-C15

Submitter Material: CHARCOAL
Analyzed Material: Charred material
Pretreatment: (charred material) acid/alkali/acid
Percent Modern Carbon: 33.98 +/- 0.25 pMC
Fraction Modern Carbon: 0.3398 +/- 0.0025
D14C: -660.17 +/- 2.54 o/oo
Δ14C: -662.91 +/- 2.54 o/oo (1950:2017)
Measured Radiocarbon Age: (without d13C correction): 8690 +/- 60 BP
Calibration: BetaCal3.21: HPD method: INTCAL13

8670 +/- 60 BP — IRMS δ13C: -26.5 o/oo

(92.3%) 7848 - 7582 cal BC (9797 - 9531 cal BP)
(1.4%) 7917 - 7898 cal BC (9866 - 9847 cal BP)
(1.0%) 7869 - 7854 cal BC (9818 - 9803 cal BP)
(0.7%) 7937 - 7927 cal BC (9886 - 9876 cal BP)

(68.2%) 7731 - 7599 cal BC (9680 - 9548 cal BP)

Beta - 467842 — KT201-C24

Submitter Material: CHARCOAL
Analyzed Material: Charred material
Pretreatment: (charred material) acid/alkali/acid
Percent Modern Carbon: 85.38 +/- 0.32 pMC
Fraction Modern Carbon: 0.8538 +/- 0.0032
D14C: -146.24 +/- 3.19 o/oo
Δ14C: -153.13 +/- 3.19 o/oo (1950:2017)
Measured Radiocarbon Age: (without d13C correction): 1290 +/- 30 BP
Calibration: BetaCal3.21: HPD method: INTCAL13

1270 +/- 30 BP — IRMS δ13C: -26.4 o/oo

(92.3%) 662 - 778 cal AD (1288 - 1172 cal BP)
(1.6%) 842 - 859 cal AD (1108 - 1091 cal BP)
(1.3%) 792 - 804 cal AD (1158 - 1146 cal BP)
(0.2%) 818 - 821 cal AD (1132 - 1129 cal BP)

(68.2%):
(39.2%) 687 - 726 cal AD (1263 - 1224 cal BP)
(29%) 738 - 768 cal AD (1212 - 1182 cal BP)

The "Conventional Radiocarbon Age" was calculated using the Libby half-life (5568 years), is corrected for total isotopic fraction and was used for calendar calibration where applicable.
The Age is rounded to the nearest 10 years and is reported as radiocarbon years before present (BP), "present" = AD 1950.
Results greater than the modern reference are reported as percent modern carbon (pMC).
The modern reference standard was 95% the 14C signature of NIST SRM-4990C (oxalic acid). Quoted errors are 1 sigma counting statistics.
Calculated sigmas less than 30 BP on the Conventional Radiocarbon Age are conservatively rounded up to 30.
d13C values are on the material itself (not the AMS d13C). d13C and d15N values are relative to VPDB-1. References for calendar calibrations:
Probability Method: Bronk Ramsey, C. (2009). Bayesian analysis of radiocarbon dates. Radiocarbon, 51(1), 337-360. Database INTCAL13: Reimer, et. al., 2013, Radiocarbon55(4).

Figure captions

Fig. 1: a) Schematic tectonic map of Myanmar depicting the epicentres of M≥6.5 earthquakes from the USGS earthquake database (website *earthquake.usgs.gov/earthquakes/search*, last access: 2019-05-05). b) Isoseismal distribution related to the 1912 Maymyo earthquake as reported by Coggin Brown (1917), based on the Rossi-Forel scale, where maximum intensity is X. c) Tectonic setting of the northern part of the Kyaukkyan Fault. The hillshade basemap is based on SRTM3. NP: Nawnghkio Plateau; KP: Kyaukku Plateau.

Fig. 2: Topographic map of trench T1 area (a), near Kyaukkyan village. b), c), d), e) Google Earth view of the Kyaukkyan Fault trace, indicated by white arrows, with location of railway bend, abandoned trenches (in c) and trenching site T1 (in d); map locations shown in Fig. 2a. f) Plot of the measured right-lateral offset of the railway bend (g), with 20x horizontal exaggeration. h) Trench T1, view to the west. Map location shown in Fig. 1c. Imagery ©2019 Google and CNES / Airbus.

Fig. 3: Schematic stratigraphic log of units identified in trench T1, with average thickness of units and stratigraphic location of the dated samples. For unit descriptions and other details see text.

Fig. 4: Orthorectified photomosaic (top) and interpretative log (bottom) of N-wall (a) and S-wall (b) in trench T1. Black dots locate the position of the charcoals collected for radiocarbon dating. Stars indicate faulting events. Colours of lithologic units correspond to those of the stratigraphic log in Fig. 3. Dashed squares indicate location of photographs in Fig. 5. For trench log descriptions and other details see text.

Fig. 5: Photos of trench T1. a) Cooking pit (dashed) with abundant charcoal, N-wall. b) Layer of bricks and centimetric fragments on its right by m 0 (vertical wire), S-wall. c) Detail of deformation observed in the platy calcrete layer B1.b along the fault plane, N-wall. d) Perspective view to the N of the truncated layers B2+B3, N-wall. White arrows indicate the fault plane.

Fig. 6: a) Topographic map of trench T2 area, north of Taunggyi. b) 2012 DigitalGlobe/Google Earth image of the lineament within the basin-filling sediments (left), and the scarp between the basin and the *terra*

rossa (right), indicated by the white arrows, with location of T2 trenching site and location of an abandoned trench. Map location shown in Fig.1b. Imagery ©2019 Google and DigitalGlobe.

Fig. 7: Orthorectified photomosaic (top) and interpretative log (bottom) of N-wall (a) and S-wall (b) in trench T2. Stars indicate faulting events. For trench log descriptions and other details see text.

Fig. 8: Photos of trench T2. a) Photograph of N-wall with modified colour balance highlighting the deformed level C1b. b) Fractured and faulted dolomitic limestone at the base of the trench, view to the west. c) Detail of fault gouge at the contact between bedrock and unit C1b, S-wall. White arrows indicate the fault planes.

Fig. 9: Map summarising the distribution of damage within the isoseismals VIII and IX of Rossi-Forel intensity scale (see Fig. 1b for reference), and other information related to the 1912 Maymyo earthquake. Text in *italics* refers to the damages reported by [1] Coggin Brown (1917). Other sources: [2] This paper; [3] Soe Min et al. (2017); [4] Vigny et al. (2003); [5] Wang et al. (2014). Locations of earthquakes from USGS earthquake database (website *earthquake.usgs.gov/earthquakes/search*, last access: 2019-05-05).

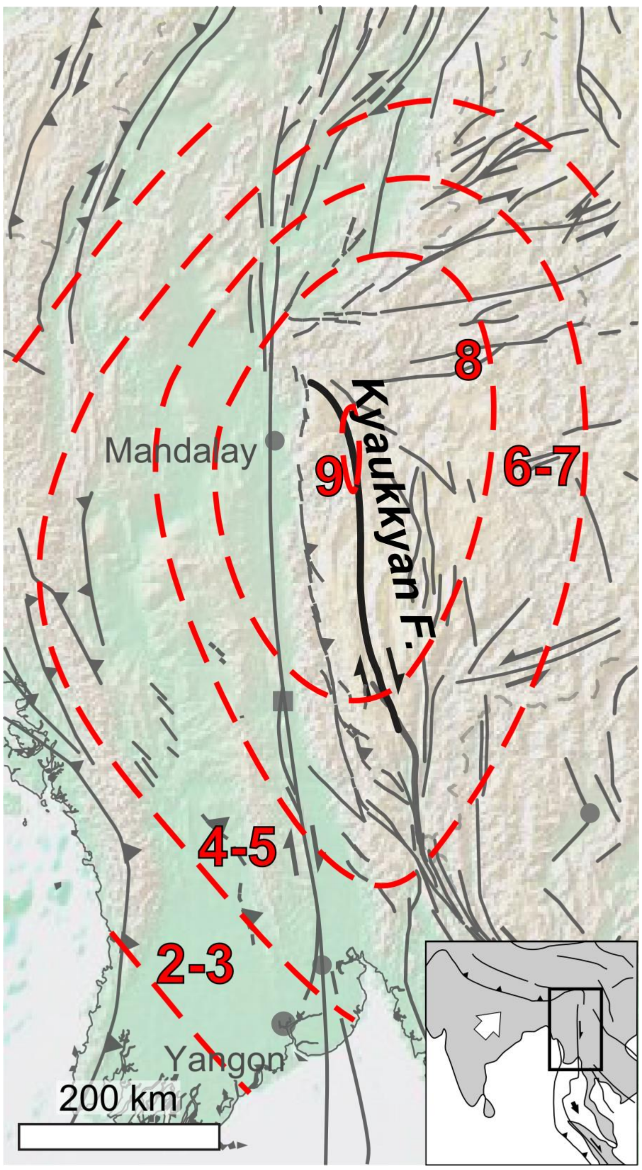

Figure 1

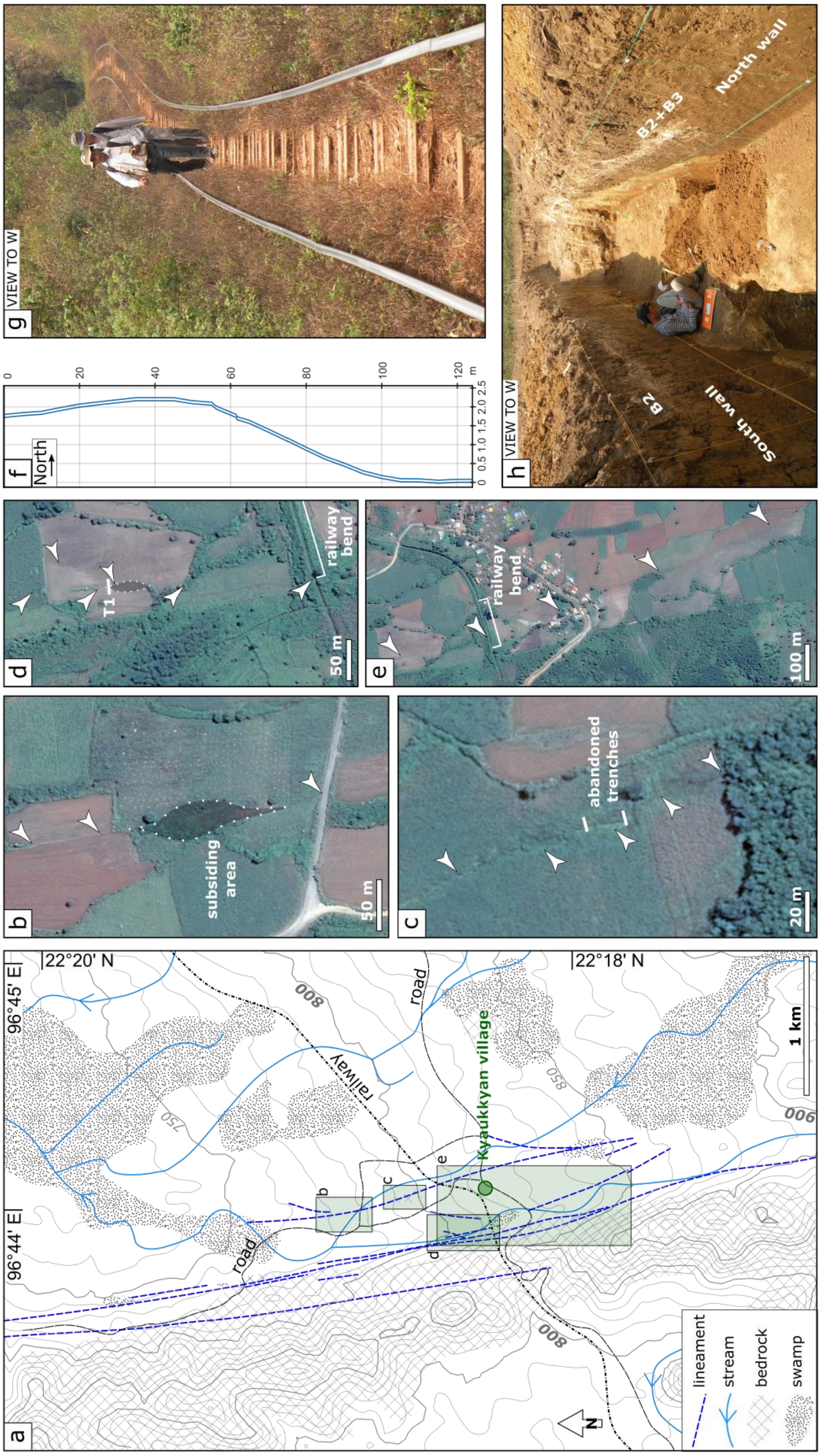
a
96°44' E
96°45' E
22°20' N
22°18' N
railway
road
Kyaukkyan village
750
800
850
900
1 km
N
lineament
stream
bedrock
swamp
b
subsiding area
50 m
c
abandoned trenches
20 m
d
T1
railway bend
50 m
e
railway bend
100 m
f
North
0
20
40
60
80
100
120
m
0.5
1.0
1.5
2.0
2.5
g
VIEW TO W
h
VIEW TO W
B2
B2+B3
South wall
North wall

Figure 2

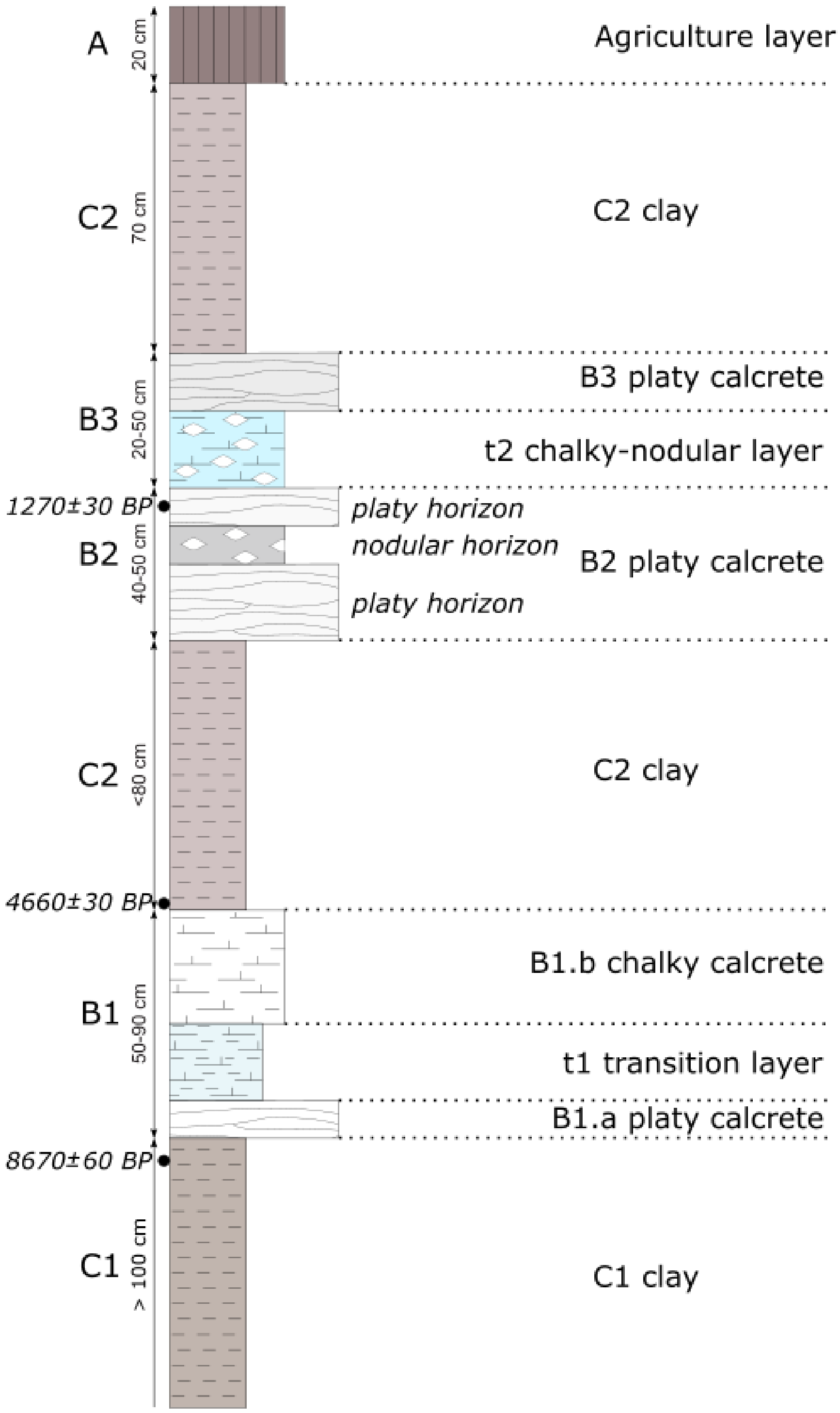
A
20 cm
Agriculture layer
C2
70 cm
C2 clay
B3
20-50 cm
B3 platy calcrete
t2 chalky-nodular layer
1270±30 BP
platy horizon
nodular horizon
B2
40-50 cm
B2 platy calcrete
platy horizon
C2
<80 cm
C2 clay
4660±30 BP
B1.b chalky calcrete
B1
50-90 cm
t1 transition layer
B1.a platy calcrete
8670±60 BP
C1
> 100 cm
C1 clay

Figure 3

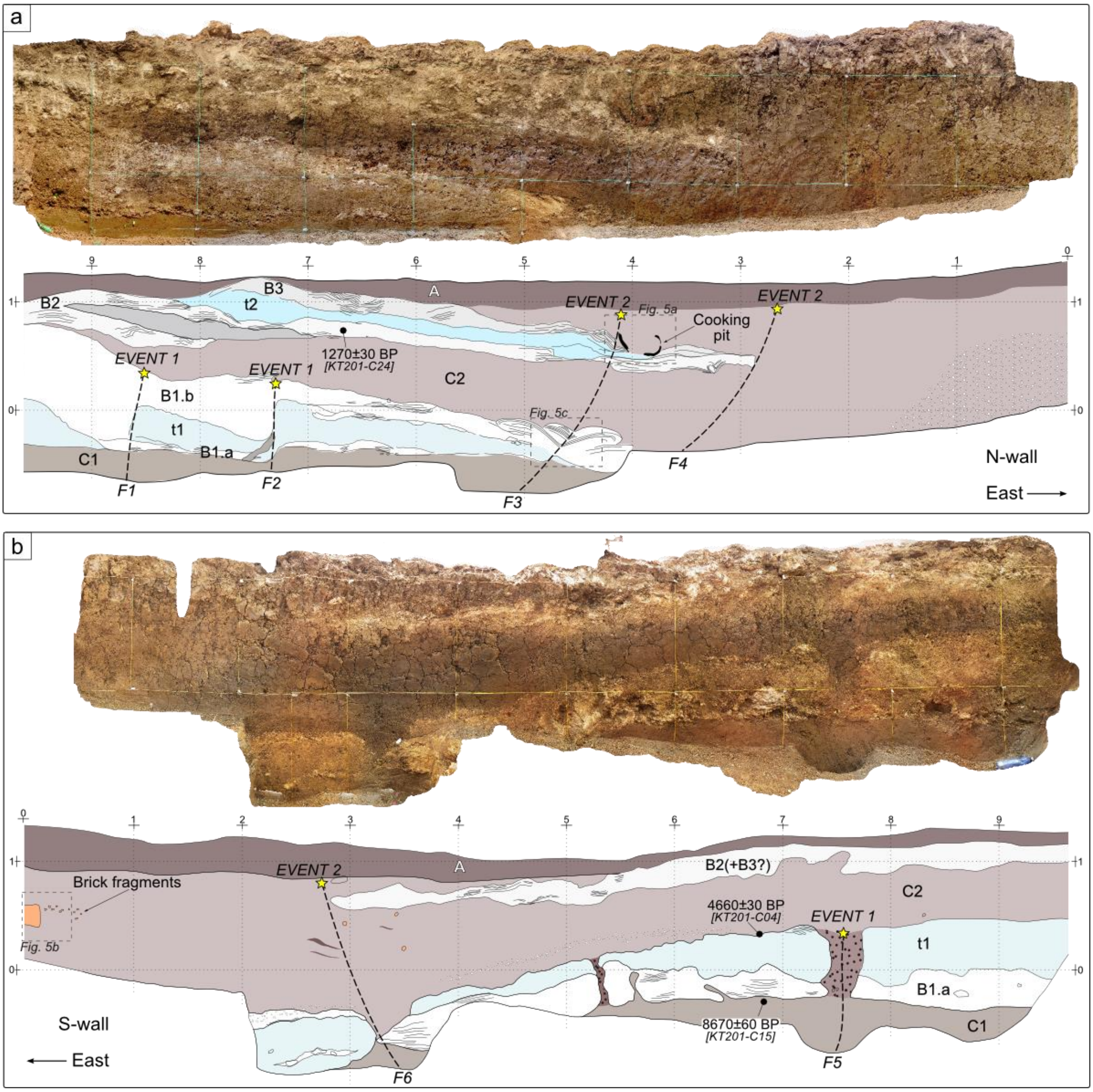
a
9
8
7
6
5
4
3
2
1
0
B2
B3
t2
A
EVENT 2
Fig. 5a
Cooking
pit
EVENT 2
1270±30 BP
[KT201-C24]
EVENT 1
EVENT 1
C2
B1.b
Fig. 5c
t1
B1.a
C1
F1
F2
F3
F4
N-wall
East
b
0
1
2
3
4
5
6
7
8
9
A
EVENT 2
B2(+B3?)
Brick fragments
C2
4660±30 BP
[KT201-C04]
EVENT 1
Fig. 5b
t1
B1.a
S-wall
8670±60 BP
[KT201-C15]
C1
East
F6
F5

Figure 4

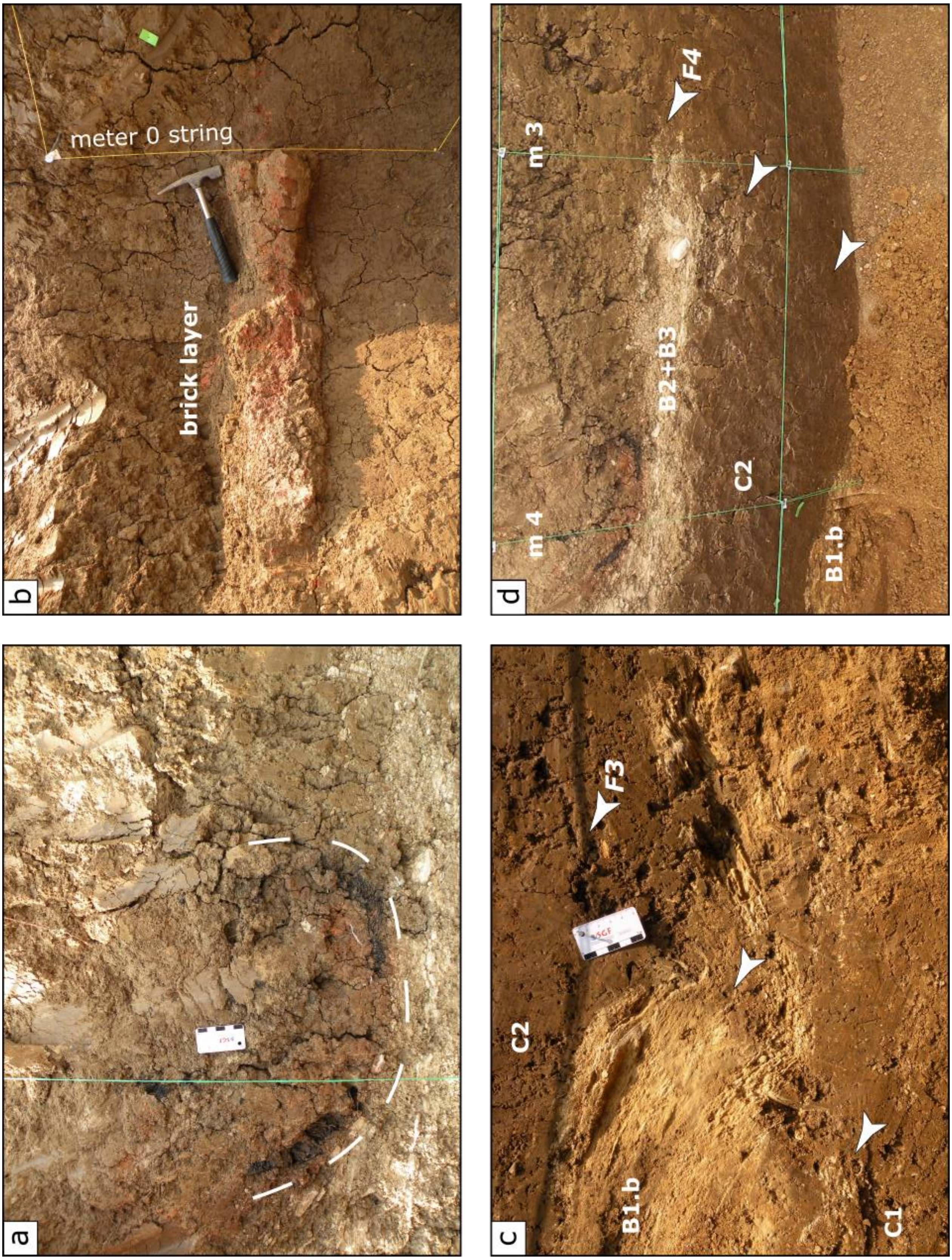
a
b
meter 0 string
brick layer
c
C2
F3
B1.b
C1
d
F4
m 3
m 4
B2+B3
C2
B1.b

Figure 5

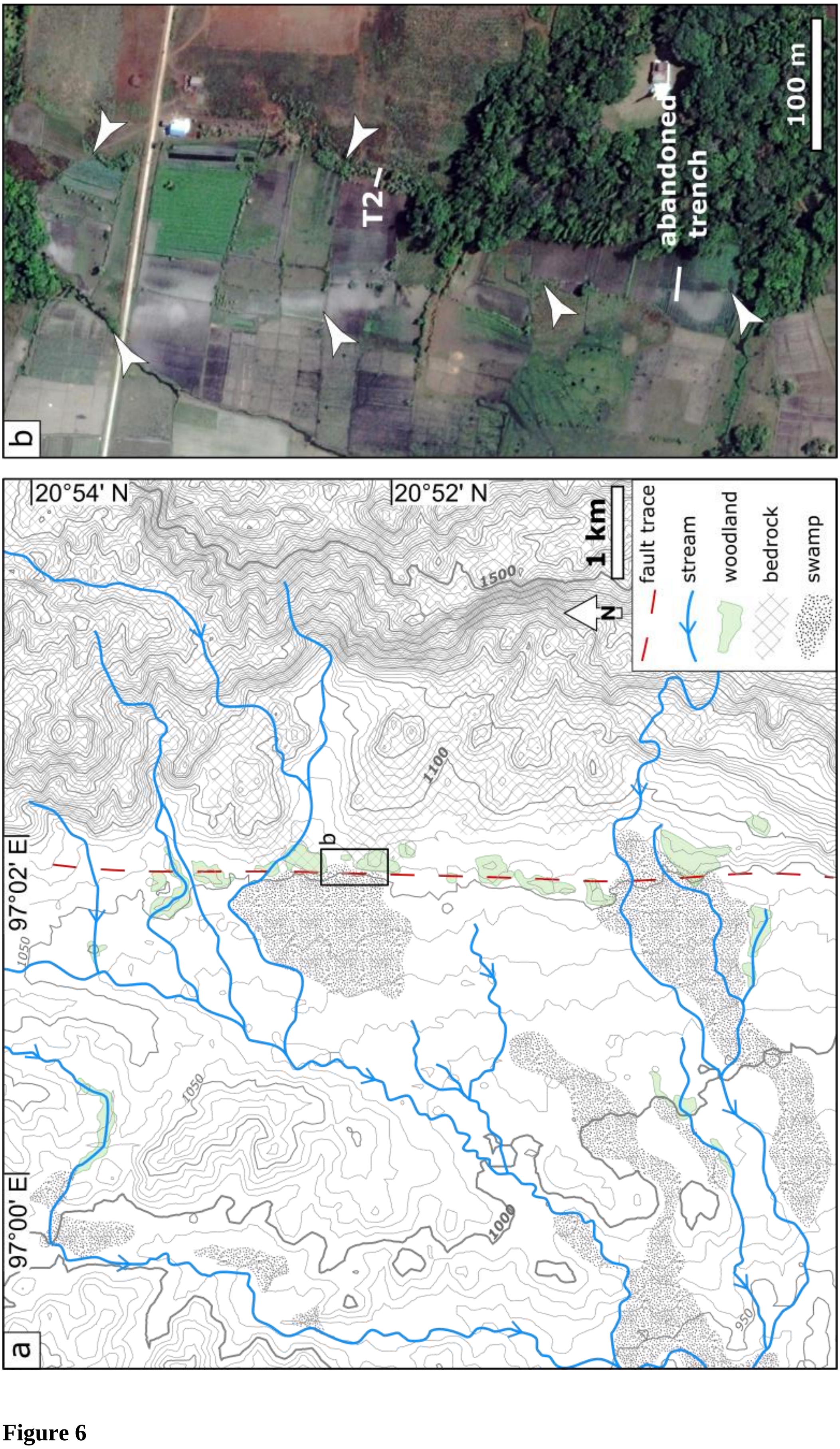
a
b
20°54' N
20°52' N
97°02' E
97°00' E
1 km
N
fault trace
stream
woodland
bedrock
swamp
1500
1100
1050
1000
950
T2
abandoned
trench
100 m

Figure 6

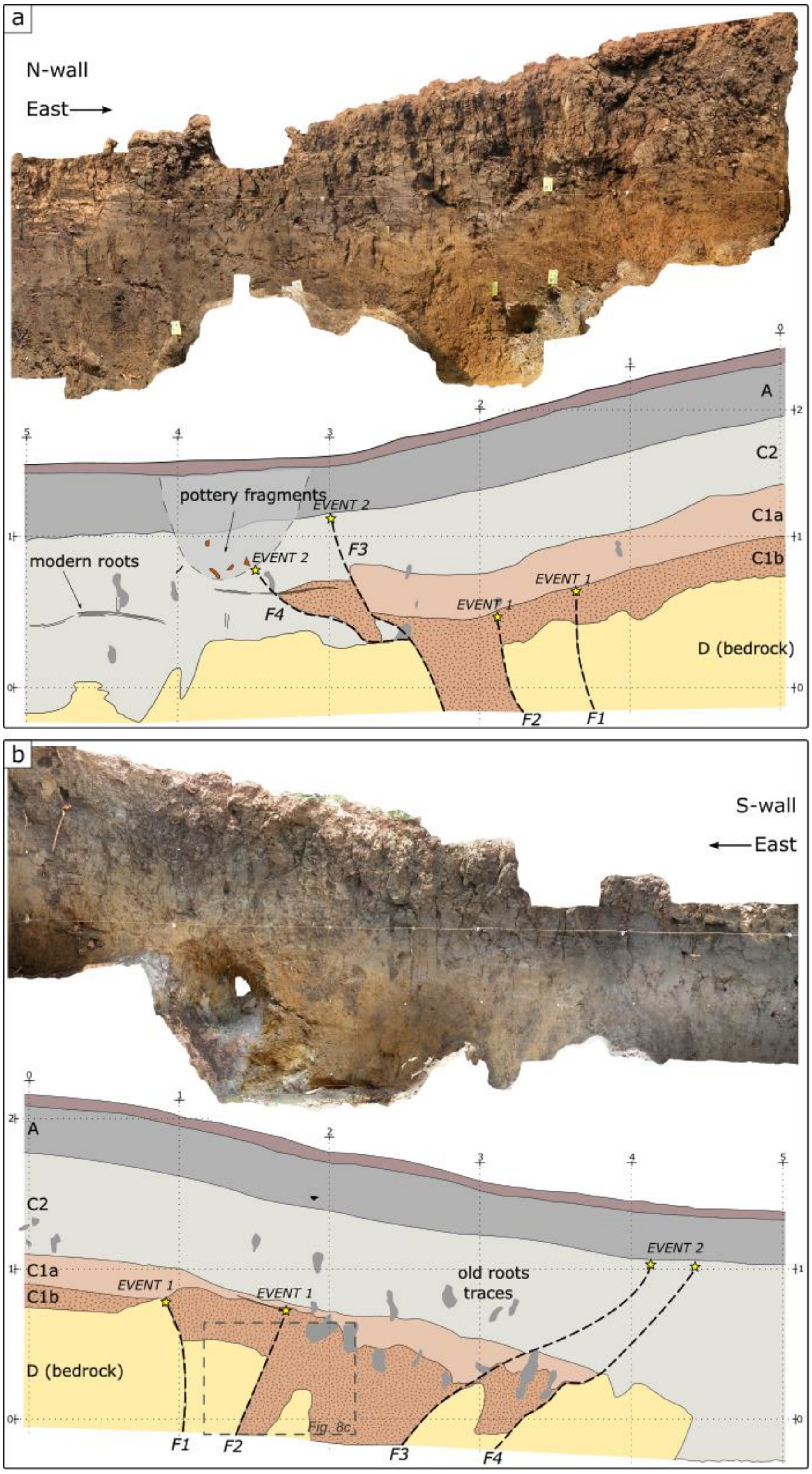
a
N-wall
East
A
C2
C1a
C1b
D (bedrock)
pottery fragments
modern roots
EVENT 2
EVENT 2
EVENT 1
EVENT 1
F1
F2
F3
F4
b
S-wall
East
A
C2
C1a
C1b
D (bedrock)
old roots traces
EVENT 1
EVENT 1
EVENT 2
Fig. 8c
F1
F2
F3
F4

Figure 7

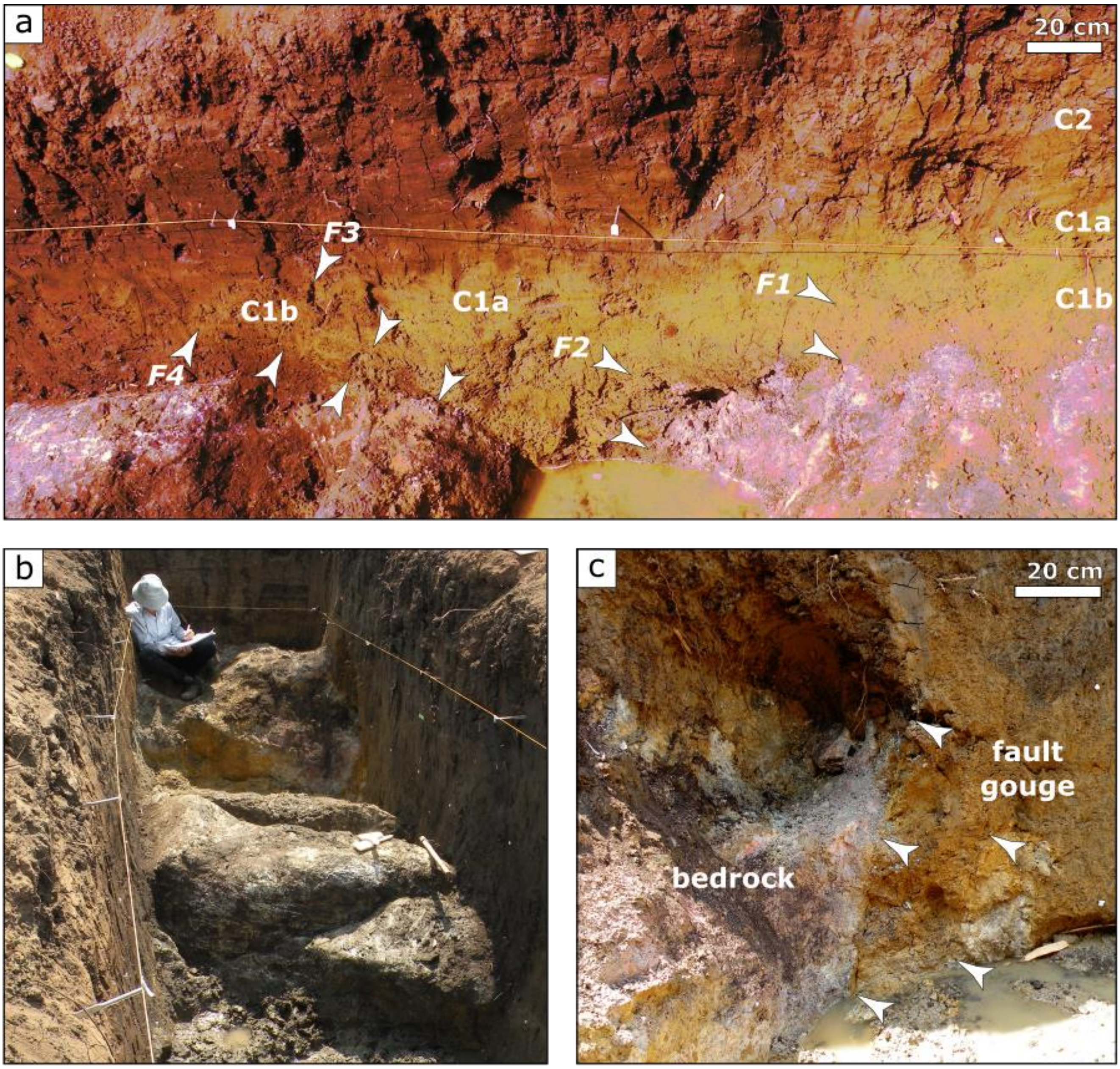
a
20 cm
C2
C1a
C1b
F3
C1b
C1a
F1
F2
F4
b
c
20 cm
fault
gouge
bedrock

Figure 8

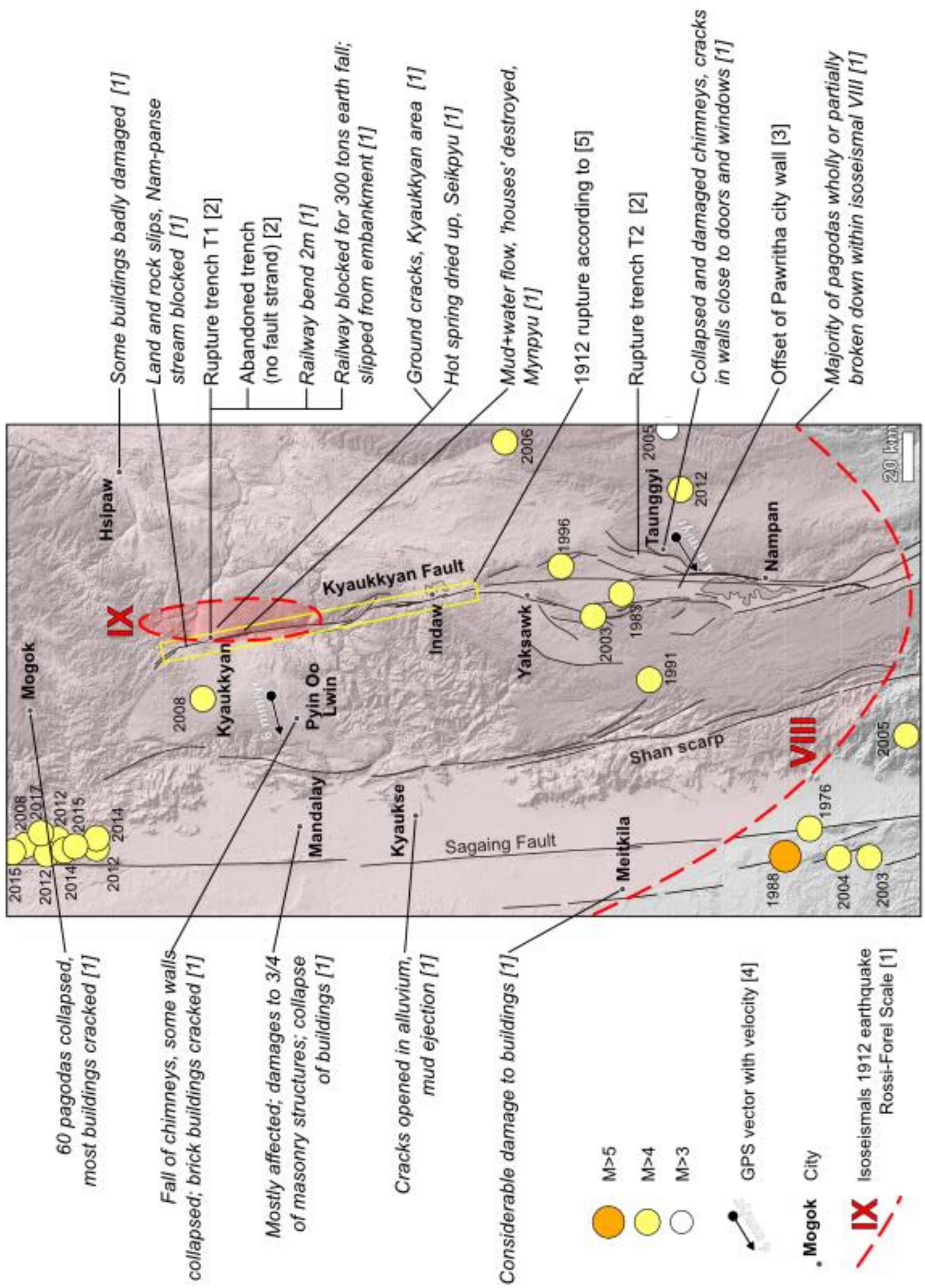
Some buildings badly damaged [1]
Land and rock slips, Nam-panse stream blocked [1]
Rupture trench T1 [2]
Abandoned trench (no fault strand) [2]
Railway bend 2m [1]
Railway blocked for 300 tons earth fall; slipped from embankment [1]
Ground cracks, Kyaukkyan area [1]
Hot spring dried up, Seikpyu [1]
Mud+water flow, 'houses' destroyed, Mynpyu [1]
1912 rupture according to [5]
Rupture trench T2 [2]
Collapsed and damaged chimneys, cracks in walls close to doors and windows [1]
Offset of Pawritha city wall [3]
Majority of pagodas wholly or partially broken down within isoseismal VIII [1]
60 pagodas collapsed, most buildings cracked [1]
Fall of chimneys, some walls collapsed; brick buildings cracked [1]
Mostly affected; damages to 3/4 of masonry structures; collapse of buildings [1]
Cracks opened in alluvium, mud ejection [1]
Considerable damage to buildings [1]
Hsipaw
Mogok
IX
Kyaukkyan
Kyaukkyan Fault
Indaw
Pyin Oo Lwin
Yaksawk
Taunggyi
Nampan
Mandalay
Kyaukse
Meitkila
Sagaing Fault
Shan scarp
VIII
20 km
M>5
M>4
M>3
GPS vector with velocity [4]
Mogok City
Isoseismals 1912 earthquake Rossi-Forel Scale [1]

Figure 9